

TA1 匹配焊接材料及其焊接接头组织的细化机理分析

张 敏, 吕金波, 吕 娜, 李继红

(西安理工大学 材料科学与工程学院, 西安 710048)

摘 要: 针对熔化温度高、热容量大等原因造成的纯钛焊接时组织粗大, 并影响到焊接接头综合性能的问题, 文中应用焊材微合金过渡来改善工业纯钛焊缝处的组织形态, 并对合金相和微观组织的细化过程进行了观察及分析。结果表明, 不同焊接工艺条件下, 合理的合金化可以达到细化工业纯钛焊缝处组织及晶粒的作用。从焊缝组织相的分布来看, 主要以 α 相、 γ 相和 TiB_2 强化质点为主; 与此同时, 在快冷条件下, 也可能产生 α' 共晶相。细针状 TiB_2 在三维空间上两两垂直相交, 成十字形、“T”形或三维空间较复杂的十字或“T”形的复合形, 分布于晶界处。

关键词: 晶粒细化; 合金化; 钛合金

中图分类号: TG421 **文献标识码:** A **文章编号:** 0253-360X(2011)06-0045-04



张 敏

0 序 言

钛由于其良好的耐腐蚀性能被广泛的选用作为电解铜箔用阴极辊的基体材料。随着钛辊体积逐渐变大, 无法采用电子束焊进行焊接, 而改用手工钨极氩弧焊(TIG)进行焊接生产, 但利用TIG焊接工艺生产的阴极钛辊焊缝处晶粒粗大, 这使得电流在阴极辊基体上与焊缝处分布不均, 导致电解铜箔在焊缝处出现光亮带^[1], 影响其表面质量及使用性能。

文中基于钛合金焊接接头的组织特点, 从焊接熔池凝固过程入手, 深入讨论合金元素对工业纯钛焊接接头组织的影响机理, 一方面对其组织进行设计, 稳定 α 相, 使其在预估的温度区间进行转化, 获得不同形态、不同比例双相组织; 另一方面根据以上研究思路细化焊缝晶粒尺寸, 并分析合金元素对焊接接头的细化机理。

1 合金成分的匹配设计

不同的合金元素对工业纯钛 TA1 焊接接头组织细化的机理如下。

(1) 铝的影响。铝具有显著的固溶强化作用,

它在 α -Ti 中的固溶度大于在 β -Ti 中的固溶度, 并提高 α/β 相互转变的温度, 扩大 α 相区, 属于 α 稳定元素。当合金中铝的质量分数在 7% 以下时, 随铝含量的增加, 合金的强度提高, 而塑性无明显降低。而当铝的质量分数超过 7% 后, 由于合金组织中出现脆性的 Ti_3Al 化合物, 使塑性显著降低, 故铝在钛合金中的质量分数一般不超过 7%。

(2) 硼的影响。硼属于表面活性元素^[2,3], 其主要作用是细化晶粒, 硼的添加可使柱状晶宽度降至 1 mm。当硼含量为 0.2% 和 0.4% 时, 等轴晶的直径分别为 20 μm 和 40 μm , 晶粒尺寸约为 1 mm。长柱状晶以长的初始枝晶和短的二次枝晶的形式生长, 晶间和枝晶间有大量 TiB 析出物。当铝含量相对较低时, 合金基体为 α -Ti, 硼化物为单一的 TiB , 铝含量增加时, 基体中形成 α_2 相及 γ 相, 并开始出现 TiB_2 , 其含量不断增加, 硼最终全部以 TiB_2 形式存在。当硼添加量达到 1.0% 时, 虽然合金锭等轴晶区增大, 但等轴晶粒尺寸未变, 而且枝晶间 TiB 体积分数高了很多, 大的 TiB 束超过了 50 μm , 与硼含量较低的合金相比, 合金锻造后再结晶程度要高得多。因此, 加入硼可使锻造后显微组织大大细化, 而且可以延缓固溶处理后晶粒的生长, 可获得较为均匀的显微组织, 这归因于晶界的齐纳钉扎效应。

(3) 碳的影响。碳的加入可以起到细化晶粒的作用^[4,5], 含量小于 0.09% 的碳完全固溶于基体中, 产生固溶强化效果, 阻碍位错运动, 同时合金仍然保

持细小的晶粒,提高了合金强度和蠕变性能.在含碳的钛合金焊缝中,随着碳含量的增加,在 β 原始晶界和晶粒内部析出碳化物.当碳含量大于0.23%时,碳对 α' 或 α 片层的影响减小.从 β 相区淬火至室温时,高温 β 相通过切变方式转变为马氏体 α' 相,形成的 α' 片贯穿 α 群体,而后通过界面的推移长大.由此表明,碳的加入细化 β 晶粒也导致 α 群体较小,因此,随着碳含量的增加 β 晶粒尺寸减小,从而间接影响 α' 或 α 片层的大小.

综合上述分析,从细化晶粒角度出发,打破传统选用纯钛焊材作为填充材料的原则,文中拟定两种焊丝合金系: Ti-Al-B(1号焊丝)、Ti-Al-C(2号焊丝).其中,硼和碳均有细化钛晶粒的作用,铝的加入可以改变钛合金焊缝熔敷金属相的组成,在细化焊缝组织的同时,提高焊缝的力学性能.两种焊丝的具体成分如表1所示.

表 1 焊丝成分(质量分数,%)

Table 1 Component and serial number of welding wire

编号	Ti	Al + B	Al + C
1 号	93.4 ~ 96.7	3.3 ~ 6.6	—
2 号	92.5 ~ 96.5	—	3.5 ~ 7.5

2 焊接试验及熔敷金属组织分析

2.1 试验材料及工艺

分别采用纯钛焊丝以及自制的两种 α 型钛合金焊丝进行焊接试验,母材为320 mm×320 mm×8 mm的工业纯钛TA1板材,其化学成分具体如表2所示.

表 2 母材 TA1 化学成分(质量分数,%)

Table 2 Composition of base metal TA1

Ti	Fe	Si	C	N	H	O
99.2 ~ 99.3	0.25	0.10	0.10	0.03	0.015	0.25

试验采用的两种焊接工艺具体参数见表3,焊接试验均采用直流反接,氩气纯度大于99.99%.平板对接焊缝为60°角V形坡口,留钝边.焊前对坡口及其周围50 mm范围内进行严格清理,焊后在接头处取样,经粗抛、精抛后用1HNO₃:1HF的腐蚀液腐蚀.

2.2 焊丝熔敷金属组织分析

图1为母材组织形貌,由均匀的 α 相等轴晶粒组成,大多呈五边形,长轴长度约为0.2 mm,短轴约

为0.12 mm,组织分布较为规律,晶界纯净,没有第二相组织,但晶粒尺寸明显偏大.

表 3 焊接参数

Table 3 Welding parameters

焊接方法	电弧电压 <i>U/V</i>	钨极直径 φ /mm	焊丝直径 <i>d</i> /mm	焊接层数 <i>n</i>	焊接电流 <i>I/A</i>
熔化极气体保护焊	16	—	1.15	3 ~ 4	140 ~ 180
手工钨极氩弧焊	—	4	3	3 ~ 4	140 ~ 180

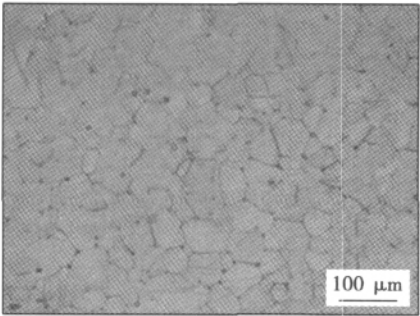


图 1 母材组织形貌
Fig. 1 Microstructure of base metal

图2为采用纯钛焊丝与文中研制的1号、2号焊丝经手工钨极氩弧焊后的熔敷金属组织形貌.图2a为纯钛焊丝熔敷金属组织形貌,属于典型的魏氏组织,晶界明显,晶粒的尺寸较母材组织更为粗大,长轴达到约2 mm,短轴约为1.8 mm,且晶内存在一定方向性的羽毛状 β 相组织;而自制两种 α 钛合金焊丝均起到了细化焊缝组织的作用,如图2b、c所示,其中1号焊丝焊缝区组织以 α' -Ti- α_2 相或 γ 相为基体,硼化物为针状或片状的TiB和块状TiB₂组成;而2号焊丝焊缝区合金相以数个或更多个呈簇聚状分布,径向尺寸大多小于3 μ m,长度多为15 ~ 40 μ m.其内部出现类似TiC相质点团,它是细化 α -Ti的有效异质结晶核心.综合比较可以发现,1号焊丝在手工钨极氩弧焊下细化效果最好,2号焊丝次之,纯钛焊丝效果最差.

图3为采用纯钛焊丝与文中研制的1号、2号焊丝在熔化极氩弧焊下熔敷金属组织形貌.图3a为纯钛焊丝焊缝区的金相组织形貌,与手工钨极氩弧焊条件下相同,也属于典型的魏氏组织,晶界明显,晶粒尺寸明显大于母材,晶内出现了羽毛状组织,而文中研制的两种焊丝熔敷金属组织形貌如图3b、c所示,较母材与纯钛焊丝焊缝组织更为细小.从图3b可以看出,1号焊丝焊缝区的细小晶粒为针状马氏体,其晶界 β 相不明显,合金相TiB₂呈簇聚状分

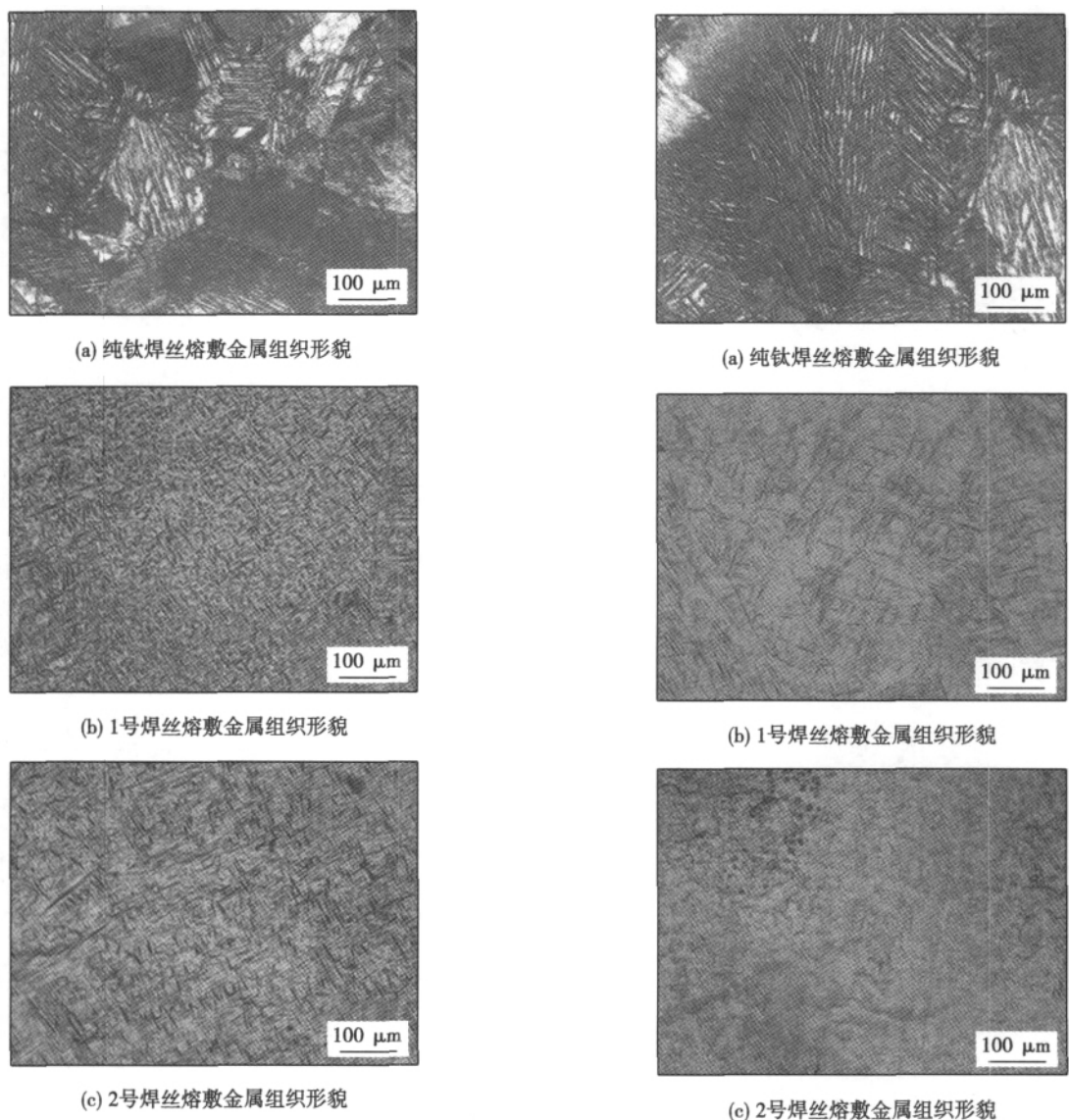


图 2 手工钨极氩弧焊下不同焊丝的熔敷金属组织形貌
Fig. 2 Microstructure of deposited metal with different welding wire by TIG

布, 径向尺寸大多小于 $3\text{ }\mu\text{m}$, 长度多为 $15\sim40\text{ }\mu\text{m}$; 而在图 3c 中 2 号焊丝焊缝区只能看到少量的针状组织, 主要以均匀分布的质点团组织为主. 综合比较可以发现, 2 号焊丝在熔化极氩弧焊下焊缝组织细化效果最好, 1 号焊丝次之, 纯钛焊丝效果最差.

3 合金元素细化机理分析

在 1 号及 2 号焊丝中加入 α 稳定元素可以扩大 α 相区, 使 β 相变点升高. 由于在 β 相中原子扩散系数大, 焊接温度一旦超过 β 相变点, 容易形成粗大组织. 当合金元素含量少, 即用纯钛焊丝焊接得到的焊接接头组织, 由于马氏体形成温度 M_s 点高, 形成块状组织, 得到板条状马氏体; 当合金元素含量增高时, 即用 1 号及 2 号焊丝焊接得到的焊接接头组

图 3 熔化极氩弧焊下不同焊丝的熔敷金属组织形貌
Fig. 3 Microstructure of deposited metal with different welding wire by MIG

织, 由于 M_s 点降低, 就会形成针状组织, 即为针状马氏体. 板条马氏体内有密集的位错, 基本上没有孪晶, 而针状马氏体内则有大量的细孪晶.

在自制焊丝的焊缝处陶瓷相 TiB_2 主要以块状、板状、细棒状或片状存在于基体 TiAl 中^[6], 细棒状 TiB_2 主要位于晶界处, 以数个或更多个呈簇聚状分布, 径向尺寸大多小于 $3\text{ }\mu\text{m}$, 长度多为 $15\sim40\text{ }\mu\text{m}$. 细棒状 TiB_2 呈相互垂直交叉的十字形、“T”字形或三维空间较复杂的十字或“T”字形的复合形^[7]. 实际上, 呈簇聚状的 TiB_2 是由较多的细针状 TiB_2 在三维空间上两两垂直相交, 交点可以位于细棒 TiB_2 六个柱面的任何一个柱面, 从而形成簇聚状.

由图 4 中 Ti-Al-B 三元合金富钛侧相图液相面投影图可知, 随着初生相 TiB_2 的析出, 熔体中 B 元素含量减少、Al 元素含量增加, 发生 $L\rightarrow\alpha+\text{TiB}_2$ (或

$L \rightarrow \gamma + \text{TiB}_2$ 的共晶反应。由于冷却速度较快,大部分初生相 TiB_2 刚完成形核过程就发生上述共晶反应,这些晶核将与共晶反应相同时长大。

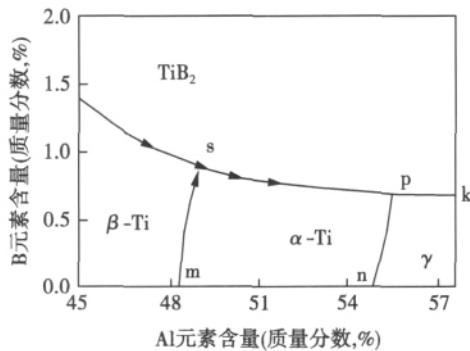


图 4 Ti-Al-B 合金富钛侧相图液相面投影面

Fig. 4 Preliminary liquidus projection on titanium rich side of Ti-Al-B ternary diagram

图 5 为 TiB_2 粒子 $[101]$ 晶带轴的衍射花样^[8]。它们的生长空间因受到 α 或 β 相的限制,使其晶体两个方向的生长速度变慢甚至停止,容易生长为板条状。当第二相体积分数含量很低时,小面生长相的形态由片状转为细棒状是很普遍的现象。在焊缝处的合金含量较少,由于焊接工艺均采用空冷,冷却速度较快,初生相最终都长成了细棒状晶体。

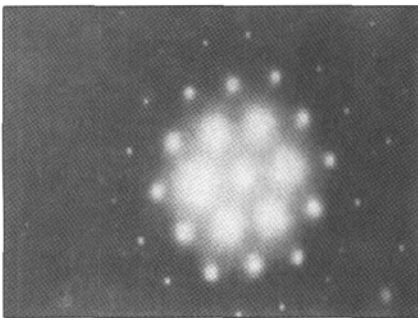


图 5 TiB_2 相粒子 $[101]$ 晶带轴的衍射花样

Fig. 5 Diffraction pattern of $[101]$ zone axis to TiB_2 particle

4 结 论

(1) 自制焊丝均能达到细化晶粒的效果,且在不同的焊接工艺条件下,优势表现不同。 α 稳定元素可以扩大 α 相区,使 β 相变点升高,其主要作用是细化晶粒。

(2) 近 α 钛合金焊丝在两种焊接工艺下,其组织主要以 α 相、 β 相和 TiB_2 为主,在快冷条件下,也可能产生 α' 相。细针状 TiB_2 在三维空间上两两垂直相交,相互垂直交叉形成十字形、“T”字形或三维空间较复杂的十字或“T”字形的复合形,分布在晶界处。

参考文献:

- [1] 王焕琴. 钛及钛合金焊接接头的组织、性能和断裂特性[J]. 焊接, 2001(11): 27-29.
Wang Huanqin. Properties, microstructure and fracture behavior of welded joints of Ti and Ti alloy [J]. Welding & Joining, 2001 (11): 27-29.
- [2] 高莹, 李德富, 于顺兵, 等. TB_2 钛合金电子束焊接接头组织与性能的试验研究[J]. 稀有金属, 2006, 30(4): 542-544.
Gao Ying, Li Defu, Yu Shunbing, et al. Microstructure and properties of TB_2 titanium alloy welded joints by electron beam welding [J]. Chinese Journal of Rare Metals, 2006, 30(4): 542-544.
- [3] 朱康英. B、C 和 Si 添加元素对 Ti-15Mo 基 β 钛合金显微组织和性能的影响[J]. 稀有金属快报, 2002, 9: 25-26.
Zhu Kangying. Effect of elements B, C and Si on microstructure and properties of β titanium alloy based on Ti-15Mo [J]. Rare Metals Letters, 2002, 9: 25-26.
- [4] Neal D F. Optimization of creep and fatigue resistance in high temperature Ti alloys IM1829 and IM1834 [J]. Titanium Science and Technology, 2005, 399(1): 222-231.
- [5] 张尚洲, 王波, 刘子全, 等. 碳对高温钛合金 Ti-60 组织和性能的影响[J]. 材料研究学报, 2007, 21(4): 433-438.
Zhang Shangzhou, Wang Bo, Liu Ziquan, et al. Effect of carbon on microstructures and mechanical properties of Ti-60 high temperature titanium alloy [J]. Chinese Journal of Material Research, 2007, 21(4): 433-438.
- [6] Hyman M E, McCullough C, Valencia J J, et al. Microstructure evolution in TiAl alloys with B additions. conventional solidification [J]. Metallurgical Transactions A, 1989, 20(9): 1847-1859.
- [7] 高文理, 张虎, 何建平, 等. Ti-Al-B 合金细棒状十字形 TiB_2 的生长特征. 稀有金属材料与工程[J]. 2003, 32(3): 179-182.
Gao Wenli, Zhang Hu, He Jianping, et al. Growth characteristic of the cruciform of TiB_2 needles [J]. Rare Metal Material and Engineering, 2003, 32(3): 179-182.
- [8] Valencia J J, Lofvander P A, McCullough C, et al. In-situ-grown reinforcements for titanium aluminides [J]. Materials Science and Engineering A, 1991, 144(12): 25-36.

作者简介: 张敏, 男, 1967 年出生, 博士, 教授。主要从事新型焊接材料、焊接结构断裂强度和焊接工程结构方面的研究。发表论文 70 余篇。Email: zhmmn@xaut.edu.cn

- 40

Abstract: Heating process of welding thermal cycle of 12% Cr stainless steel was reproduced with Gleeble 3800 thermo-mechanical simulators. Microstructure transformation, grain growth and precipitating phases were investigated with optical microscope, field emission scanning electronic microscope (FE-SEM) and transmission electron microscope. The following conclusions have been drawn. That the microstructure is almost fully austenite while the heating temperature is above 900°C. This austenite transforms to martensite during the cooling process and is retained down to room temperature. When heating temperature is higher than 1 250 °C, the austenite is completely transformed to delta ferrite. The grains slightly grow when heating temperature is below 1 250 °C. At the other hand, if the heating temperature is above 1 250 °C, grains are dramatically coarsened with an increase of peak temperature and holding time. Grain growth is effectively inhibited by the existing second phase. There are large numbers of finely dispersed complex carbides containing Nb and Ti in base metal matrix. As heating temperature is up to 1350°C, these carbides are dissolved into matrix. Therefore, the pinning grain boundaries and inhibiting grain growth effects of fine particles disappear.

Key words: ferritic stainless steel; heat affected zone; grain growth; precipitated phase

Molecular dynamic simulation of interface diffusion behavior during melting joining of thermoplastic polymer

FENG Yuqi¹, LUO Yi^{1,2}, SUN Yibo¹, WANG Xiaodong^{1,2}, ZHANG Miaomiao¹ (1. Key Laboratory for Precision and Non-traditional Machining Technology of Ministry of Education, Dalian University of Technology, Dalian 116024, China; 2. Key Laboratory for Micro/Nano Technology and System of Liaoning Province, Dalian University of Technology, Dalian 116024, China). p 41 - 44

Abstract: Interfacial diffusion behavior during melting joining of thermoplastic polymer was studied using molecular dynamic simulation method. Two-layer cell interface comprising model for polymethyl-methacrylate (PMMA) was constructed. Under different temperatures and pressures, interfacial molecular chains motion was simulated using constant temperature and pressure (i. e. NPT) ensemble, diffusion coefficient of total atom of PMMA interface system, interfacial diffusion depth and binding energy were calculated, and influencing rule of factors such as temperature and pressure to interface diffusion behavior was analyzed. Simulated results show that by heating or pressing atoms diffusion speed was improved, interfacial diffusion depth was increased by higher pressure, more interfacial binding energy was gained by higher pressure. The simulation results agreed well with the macro hot-embossing experiments, and revealed the molecular diffusion behavior between PMMA interfaces during melting joining from molecular size.

Key words: molecular dynamics; thermoplastic polymer; interface diffusion; diffusion coefficient

Welding material for TA1 and structure refining of its welded joint

ZHANG Min, LÜ Jinbo, LÜ Na, LI Jihong

(School of Material Science and Engineering, Xi'an University of Technology, Xi'an 710048, China). p 45 - 48

Abstract: Due to the high fusion temperature and large thermal capacity, the pure titanium always has coarse grain which makes poor properties of welded joint. In this paper the structure of welded joint was improved by micro-alloy transition, and the alloy phase and microstructure were analyzed. The results showed that for different welding procedures, proper alloying can refine the structure and grains of commercial pure titanium welded joint. In terms of the distribution of structure, the basic microstructures of welded joint were α , γ and strengthening particle TiB_2 , and the eutectic phase α' might appear under the condition of rapid cooling. The thin needles TiB_2 existed at grain boundary with the forms of cruciform, T shape and the composition of cruciform and T shape.

Key words: refining grain; alloying; titanium alloy

Structure optimization of T-nozzle in hydrogenated reactor

JIANG Wenchun¹, YANG Bin¹, ZHANG Yucai¹, GONG Jianming² (1. College of Mechanical and Electronic Engineering, China University of Petroleum, Dongying 257061, China; 2. School of Mechanical and Power Engineering, Nanjing University of Technology, Nanjing 210009, China). p 49 - 52

Abstract: T-nozzle is the inlet of the mixture gas of hydrogen and steam in a hydrogenated reactor. Many cracks have been generated in T-nozzle, which are caused mainly by the welding residual stresses. Finite element method is used to study the welding residual stress in T-nozzle of hydrogenated reactor. Based on considerations of residual stress, the welding structure of T-nozzle is optimized. The axial of T-nozzle is welded in the direction of head radius, through which the stress concentration is decreased. Large residual stresses are generated in the internal surface of nozzle and head, which have great effect on stress corrosion cracking. A flanging is inserted into the nozzle to isolate the residual stress from the mediums, which can prevent the stress corrosion cracking. It can be a reference for crack treatment and structure optimization of T-nozzle for hydrogenated reactor.

Key words: hydrogenated reactor; T-nozzle; residual stress; optimization

Effects of weld profile on electron beam welding residual stress distribution

FU Wei¹, HUANG Guogang¹, YANG Xinhua¹, HU Shubing², XIAO Jianzhong² (1. School of Civil Engineering and Mechanics, Huazhong University of Science and Technology, Wuhan 430074, China; 2. School of Materials Science and Engineering, Huazhong University of Science and Technology, Wuhan 430074, China). p 53 - 56, 60

Abstract: The section of weld was simplified as isosceles trapezoid. ANSYS software was used to simulate the residual stress field in TC4 titanium alloy plate with variable time step method. The effects of volume and shape of weld on welding residual stress distribution were studied while the volume was controlled by the trapezoid median and the shape by the angle of the trapezoid leg with respect to the vertical direction. It is showed that, for a constant volume, the maximum equivalent residual